Liquid Crystals
Publication details, including instructions for authors and subscription information:
http://www.informaworld.com/smpp/title~content=t713926090

Polarization and dielectric properties of an antiferroelectric liquid crystal

J. W. O'Sullivan; J. K. Vij; H. T. Nguyen

Online publication date: 06 August 2010

To cite this Article O'Sullivan, J. W. , Vij, J. K. and Nguyen, H. T.(1997) 'Polarization and dielectric properties of an antiferroelectric liquid crystal', Liquid Crystals, 23: 1, 77 — 86
To link to this Article: DOI: 10.1080/026782997208695
URL: http://dx.doi.org/10.1080/026782997208695

LIQUID CRYSTALS, 1997, VOL. 23, NO. 1, 77–86

Polarization and dielectric properties of an antiferroelectric liquid crystal

by J. W. O'SULLIVAN, J. K. VIJ*
Department of Electronic and Electrical Engineering, Trinity College, University of Dublin, Dublin 2, Ireland

and H. T. NGUYEN
Centre de Recherché Paul Pascal, Ave. A. Schweitzer, 33600 Pessac, France

(*Received 31 October 1996; accepted 3 February 1997*)

The spontaneous polarization and dielectric properties of a new antiferroelectric liquid crystal (AFLC) exhibiting several intermediate phases between the SmC_A and SmC* phases are investigated. A low frequency *ferri* Goldstone mode and a higher frequency *ferro* Goldstone mode have been observed over a certain range of temperatures. The effect of d.c. bias voltage on these modes is examined. The results confirm the existence of an FiLC phase with $q_T > 1/2$ between SmC_γ and SmC*. These also show the co-existence of the FiLC phase with SmC* over a narrow range of temperatures above the FiLC phase. The phase sequence for this material is found to contain SmC_A, SmC_γ, FiLC, (FiLC coexisting with SmC*), SmC*, SmA phases on heating and SmA- SmC* SmC_γ- SmC_A- phases on cooling.

1. Introduction

In antiferroelectric liquid crystals (AFLCs) there exist two fundamental phases, the low temperature antiferroelectric phase SmC_A and the higher temperature ferroelectric phase SmC* [1, 2]. The intermediate mesophases occurring between these two states appear due to the competing effects which stabilize the antiferroelectric and ferroelectric phases. The Ising model can predict the existence of the experimentally observed intermediate phases. In the case of the temperature induced devil's staircase, the phase structure is characterized by a parameter q_T, which describes the extent of ferroelectric ordering, where $q_T = m/n$; m denotes the number of pairs of dipoles with ferroelectric ordering and n is the total number of ferroelectric and antiferroelectric orderings within a pitch of the ordered arrangement. The field induced staircase causes $\mathbf{P}_S$ to increase monotonically with the bias field. The phase structure is described by the parameter q_E, where $q_E = R/(R + L)$; here R and L represent the numbers of molecules tilted towards the right and to the left, and the tilt angle in these two cases may not be exactly the same. The stable phases under bias field occur as a result of competitions between the temperature and field induced devil's staircases. In this paper, we report results on the spontaneous polarization, and on the dynamics of collective and molecular modes using dielectric spectroscopy in an antiferroelectric liquid crystal material synthesized recently. The chemical formula of the AFLC material is given below:

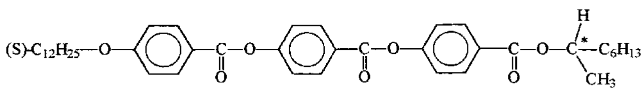

The phase sequence was obtained using a Perkin Elmer DSC 7 operated in its modulation mode. The DSC trace is shown in figure 1. The transition temperatures in °C are found to be Cr 65 SmC_A 98·5 Fi1 101 Fi2 103 SmC* 118 SmA 130 I. Wide thermal hysteresis (about 30°C) has been found between the heating and cooling cycles, especially at the SmC_A–Cr phase transition. Fi1 and Fi2 are two unknown phases and these are being characterized using polarization and dielectric measurements. There are also small peaks at 106 and 110·5°C on the heating cycle in the DSC thermogram. This aspect of the DSC trace will also be mentioned later.

2. Experimental

The liquid crystal cell consisted of two parallel indium tin oxide (ITO) coated glass plates with an active electrode area $A = 5\,\text{mm}^2$. A small electrode area was used to minimize the effects of the thickness gradient in the cell and thus ensure a uniform electric field across the sample. The glass plates were separated using mylar spacers of varying thicknesses, e.g. $d = 8$, 20, 50 μm. The

*Author for Correspondence.

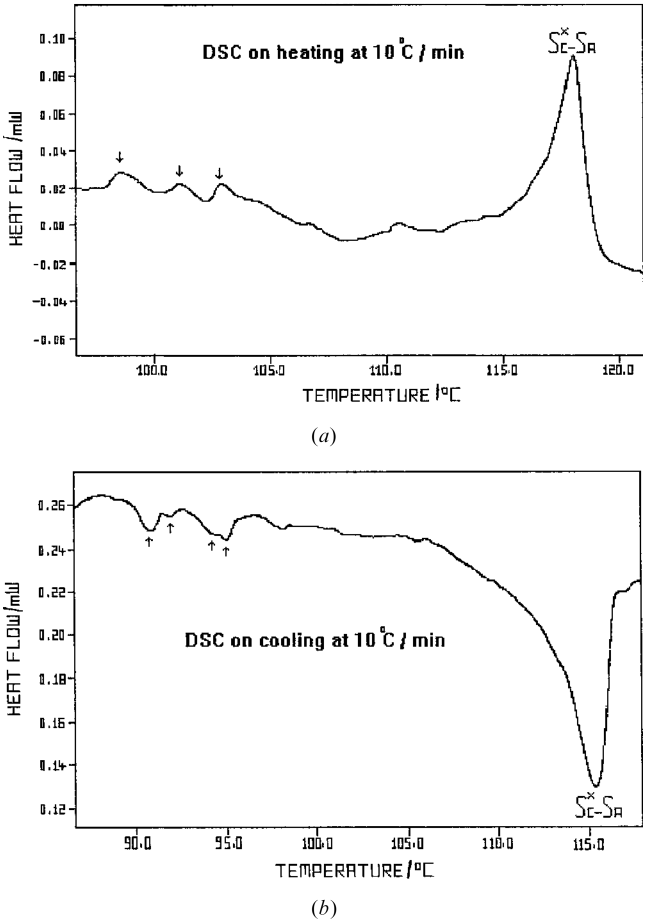

Figure 1. Heat flow versus temperature, obtained using differential scanning calorimmetry (DSC) for (*a*) heating and (*b*) cooling cycles at a temperature ramp rate of $10°C\,min^{-1}$.

ITO electrodes were coated with polyvinyl alcohol (PVA), baked for 2 hours at $T=160°C$ and subsequently rubbed unidirectionally on a velvet track. The rubbed PVA layer helps to achieve a good planar alignment. The cell was filled in the isotropic phase by capillary action. Spontaneous polarization measurements were carried out using the integral current reversal technique [3]. The sample was placed on a hot-stage of the microscope to allow visual observations of phase changes using polarizing microscopy during the spontaneous polarization measurements. A Schlumberger 1255A impedance analyser with a Chelsea dielectric interface was used for dielectric measurements in the frequency range 1 Hz to 1 MHz. This allowed the real and imaginary parts of the complex dielectric permittivity (ε', ε) to be measured as a function of frequency. The experimental set-up allowed a direct bias voltage (0 to 30 V) to be applied across the cell during dielectric measurements. The dielectric measurements and sample temperature ($\pm 0{\cdot}1°C$) were computer controlled. The relative dielectric permittivity (ε', ε) data were fitted to the Havriliak–Nagami [4] equation. The parameters $\Delta\varepsilon$, f (Hz) can then be determined from the fitted curves. Using a fitting program (DK36) it is possible to subtract the d.c. conductivity which causes ε to increase linearly with decreasing frequency (f) in the $\log\varepsilon$ $-\log f$ plots.

3. Results and discussion

3.1. *Spontaneous polarization measurements*

In the absence of a bias field and at temperatures, $T=90$, 93, 95, 98°C, the antiferroelectric phase SmC_A is the stable phase. The layer ordering of this antiferroelectric phase, as shown before, can be represented by the irreducible rational number q_T, with $q_T=m/n=0$, m and n having been defined before [1, 5].

Figure 2 shows the normalised value of P_S versus the applied electric field across the cell. Interestingly, this shows that at $T=98°C$ and for a bias field, $\mathbf{E}<0{\cdot}75\,V\,\mu m^{-1}$, the spontaneous polarization is zero, indicating that the antiferroelectric phase SmC_A with $\mathbf{P}_S=0$ $q_T=0$ and $q_E=1/2$ is the stable phase. When the field is increased, a linear increase in the spontaneous polarization is obtained. This indicates that new structures with $q_E>1/2$ are being formed. The competition between the field induced and the temperature induced staircases is made evident by a sharp jump in the spontaneous polarization, indicating that a new ferrielectric phase is formed; this new ferrielectric phase is labelled as a field induced FiL ($q_E<2/3$) phase and its occurrence is not repeated in the temperature induced staircase. This phase is also stable only over a narrow range of voltages. Further increasing the applied electric field causes the spontaneous polarization ($\mathbf{P}_S$) to make another sharp jump to a polarization of 1/3 of the maximum value (unwound SmC*) which corresponds to a stable field induced ferrielectric phase ($q_E=2/3$ and with the same structure as $q_T=1/3$). This ferrielectric phase is labelled SmC_γ. The next region involves small stepwise increases in $\mathbf{P}_S$ due to field induced metastable states, at higher fields, the SmC* phase in its distorted state is formed. For fields $\mathbf{E}$ $2{\cdot}5\,V\,\mu m^{-1}$ (T 93°C) the distorted SmC* helix is fully unwound. The spontaneous polarization reaches a saturation value and the maximum polarization for SmC* phase is obtained as $\mathbf{P}_S=1$. The phase transitions observed on increasing the applied field at $T=98°C$ are SmC_A–FiL–SmC_γ–SmC*. When the field is decreased, a hysteresis is observed in the spontaneous polarization measurements. This observation shows the existence of domains and/or irreversible field induced changes in the structure. At lower fields the spontaneous polarization decreases smoothly from the SmC_γ phase to the SmC_A phase without any sharp transitions and without exhibiting the FiL phase. This indicates that the field induced staircase is governing the structural behaviour, i.e. the new field induced regions

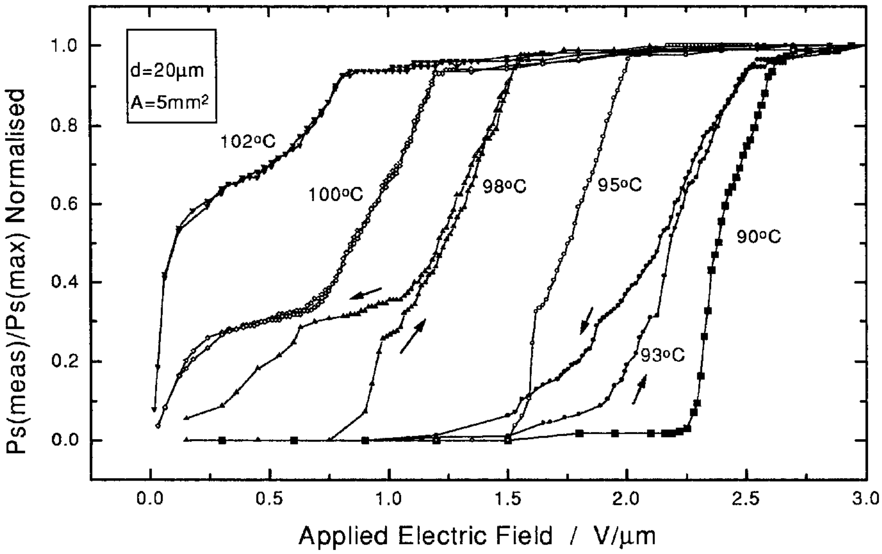

Figure 2. Normalized spontaneous polarization for different temperatures and applied field for a sample of thickness $d = 20\,\mu\mathrm{m}$. A rectangular shaped applied voltage at 50 Hz was used.

are formed due to a decrease in the ratio of molecules tilted to the right (R) to the total number ($R + L$) as the field is decreased. Here we assume the dipole moment of the molecule tilted to the right is aligned with the applied field. Using this model, it can easily be shown that the spontaneous polarization for this state is given by $(R - L)/(R + L)$.

At $T = 93°\mathrm{C}$, the hysteresis between $\mathbf{P}_S$ measured for increasing and decreasing the field is much narrower. This is due to an increased stability of the antiferroelectric ordering at this temperature. At this temperature, the temperature induced devil's staircase is driving the transition from SmC* to the antiferroelectric phase $\mathrm{SmC_A}$ and this is stronger than the competing field induced staircase which tries to force $\mathbf{P}_S$ to decrease monotonically with decreasing field. The examples shown here for temperatures of 93 and 98°C exhibit different competing effects between the field and temperature induced devil's staircases.

At $T = 100°\mathrm{C}$ the stable phase is the ferrielectric $\mathrm{SmC_\gamma}$ phase, since an application of a field $\mathbf{E} > 0{\cdot}25\,\mathrm{V\,\mu m^{-1}}$ causes this state to unwind and reach $\mathbf{P}_S = 1/3$ of the maximum value, a characteristic of this phase. In the DSC trace, the phase at this temperature was labelled as Fi1 phase. This phase is stable over an electric field range of $0{\cdot}5\,\mathrm{V\,\mu m^{-1}}$. This proves the existence and stability of this thermodynamically stable phase. A further increase in the applied electric field transforms this phase to a SmC* distorted helical state. For an applied field $\mathbf{E}$ $1{\cdot}2\,\mathrm{V\,\mu m^{-1}}$, the ferroelectric helix is completely unwound leading to a maximum value of the spontaneous polarization. On reversing the applied field at this temperature, no hysteresis in $\mathbf{P}_S$ versus field is observed due to the existence of stable structures both in the SmC* and $\mathrm{SmC_\gamma}$ phases. This behaviour is also observed for the reason that there are now no competing AF structures present at this temperature.

At $T = 102°\mathrm{C}$ the sample exhibits an unusual phase; we label this as the FiLC phase with a q_T parameter greater than 1/2 because $q_T = 1/2$ gives the AF phase above the $\mathrm{SmC_\gamma}$ phase. In the DSC trace, the phase at this temperature was designated as Fi2 phase. Most interestingly, $\mathbf{P}_S$ rises rapidly with bias to about 0·6 of the maximum value. This metastable state corresponds to a q_E of 4/5 on the field induced devil's staircase; the structure of this phase is very similar to that of $q_T = 3/5$ (see figure 3). With a further increase in the bias field, this phase transforms readily to a distorted helical SmC* phase. We propose that at this temperature and in the absence of a bias field, the structure is one with $q_T = 3/5$; however under bias the polarization $\mathbf{P}_S$ goes rapidly to 0·6, which belongs to a field induced $q_E = 4/5$. Since we do not observe a stable value of spontaneous polarization of 1/5 corresponding to a q_T of 3/5, we presume that the structure of this phase is rather unstable and under bias is easily convertible to that of $q_E = 4/5$. This also follows from the Ising model since the stability of a phase decreases with an increase in its value of q_T for 1/2 q_T 1. Because of the structure being unstable and the fact that this phase borders SmC* phase, a part of it is also easily convertible through thermal fluctuations to that of SmC* phases. The FiLC phase has recently been discovered in two other antiferroelectric liquid crystals [6–8]. It has also been found that the FiLC phase coexists with SmC* phase [8, 15] over a certain range of temperatures. In this material too, we find the existence of an FiLC phase over the temperature of the $\mathrm{SmC_\gamma}$ phase and also observe a coexistence of the two phases from the $\mathbf{P}_S$ measurements in the region $103°\mathrm{C} < T < 106°\mathrm{C}$. The observation of a small peak at 106°C may

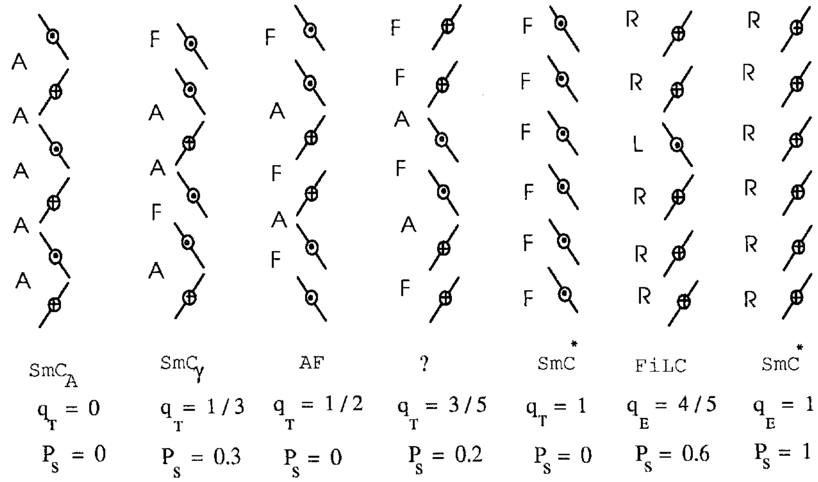

Figure 3. The molecular orderings and q_T parameters of phases on the temperature induced devil's staircase predicted by the Ising model (on heating). The P_S values represent the spontaneous polarization normalized with respect to saturation polarization for SmC*; the field induced FiLC and SmC* phases ($q_E=4/5$ and $q_E=1$, respectively) are also shown. The + and O symbols, represent the direction of the molecular dipoles out of and into the plane of the page; L and R refer to the left and right handed tilts of the molecules in adjacent layers.

imply the end of the coexistence of these phases. These findings are also supported by dielectric measurements.

3.2. *Dielectric measurements*

3.2.1. *SmC_A phase (below 69°C < T < 98·5°C)*

By definition the antiferroelectric phase, SmC_A, has no net spontaneous polarization, due to an effective cancellation of the dipole moments of adjacent layers. Two weak relaxation processes are found in the SmC_A phase [9]. The first is labelled as *Process A*, centred at a frequency of 10 kHz. The other is labelled as *Process B* centred at 300 kHz (see figure 4). The dielectric strength of *Process B*, is lower than that of *Process A*. The superposition of a peak caused by the resistance of indium/tin oxide (ITO) thin layer in series with the sample capacitance at the high frequency end of the spectrum on *Process B* implies that the latter cannot easily be resolved. The relaxation frequency of *Process A* increases only slightly with increasing temperature above the phase transition temperature as shown in figure 4. *Process A* is probably the 'antiferroelectric-like' Goldstone mode, as it occurs at the same frequency as that found for other materials and perhaps is the same as *Process A* reported previously in a different material [10]. Due to the complexity of analysis of these modes (with bias voltage) these will be discussed in a subsequent paper.

3.2.2. *SmC_γ phase (99°C < T < 101°C)*

In the temperature range 99°C < T < 101°C, a single mode of relatively weak dielectric strength of $\Delta\varepsilon_{ferri} \approx 10$ and of frequency about 200 Hz is observed (figure 5 (*a*) and 5 (*b*). Under a small applied electric field its $\mathbf{P}_S$ value

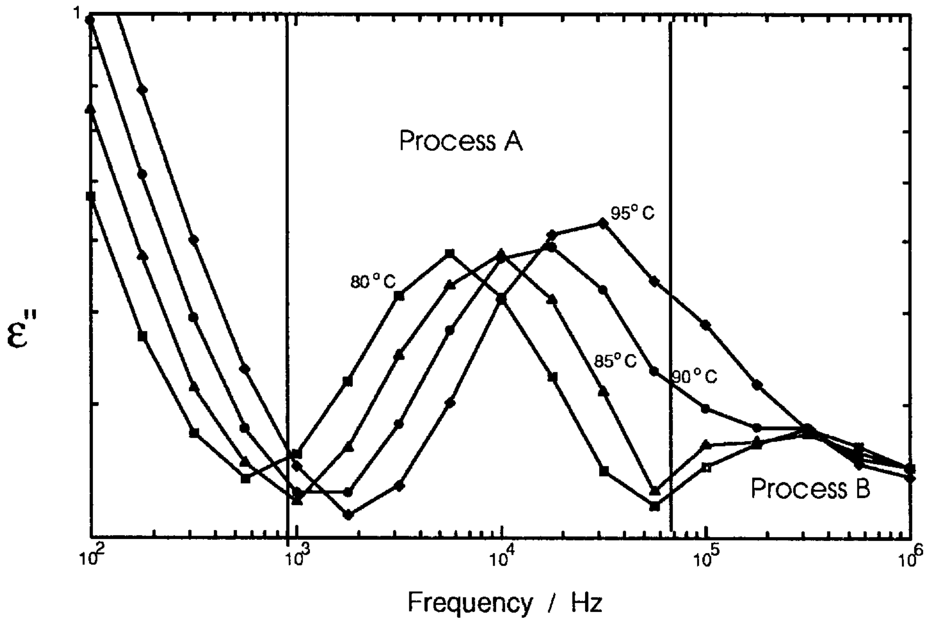

Figure 4. Dielectric loss ε versus frequency for different sample temperatures in the SmC_A phase. The antiferroelectric loss modes are labelled as *Process A* and *Process B*.

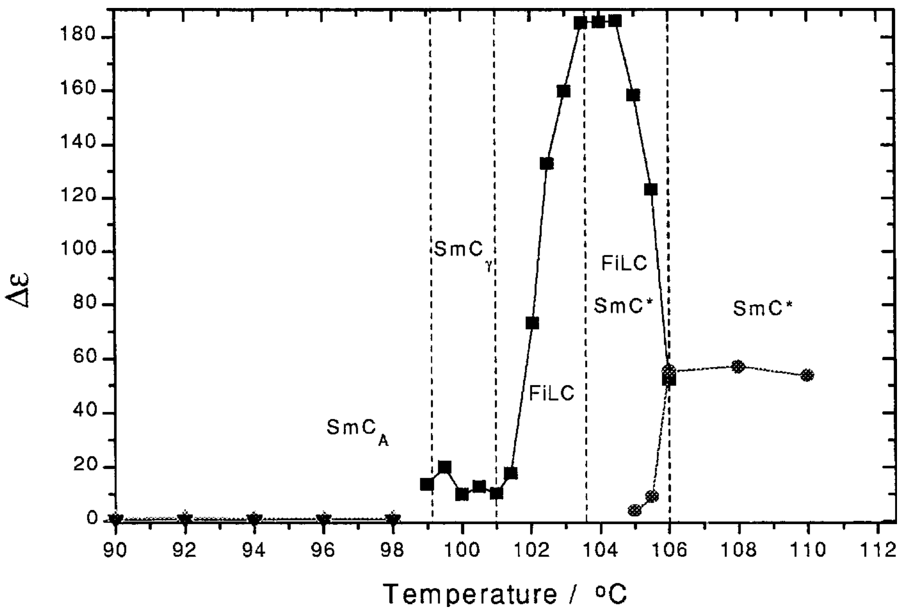

(*a*)

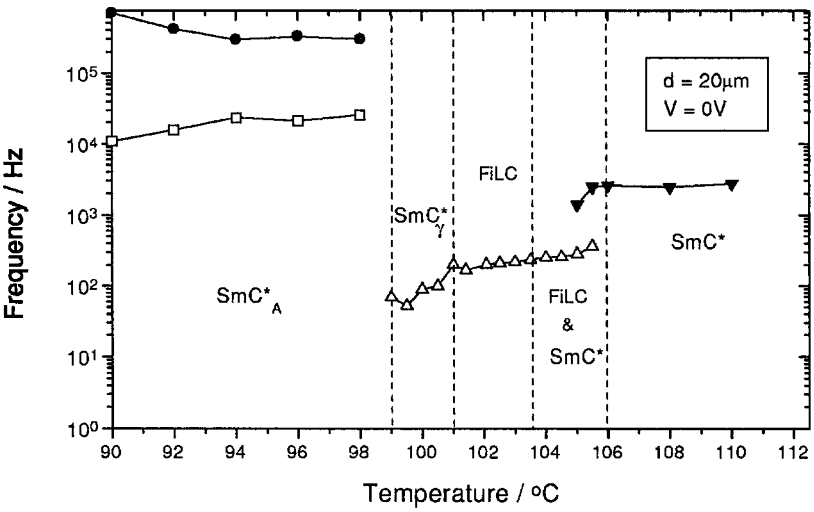

(*b*)

Figure 5. (*a*) Dielectric strength $\Delta\varepsilon$ versus temperature obtained from fitting the data to the Havriliak–Nagami equation. (*b*) Relaxation frequency versus temperature, two loss modes (*Process A*, *Process B*) are observed in the SmC_A phase. A *ferri* Goldstone mode is observed in the ferrielectric phases at a frequency $f = 200$ Hz and a *ferro* Goldstone mode is observed in SmC* phase at $f \approx 3$ kHz. In SmC_A phase Process A: □, Process B: ●.

is almost constant over a range of applied voltages and its normalized value is 0·33. This phase has therefore been assigned as the SmC_γ phase with structure parameter $q_T = 1/3$ and the mode so observed is called the *ferri* Goldstone mode. The *ferri* mode exhibits a small increase in the dielectric strength at the SmC_A–SmC_γ phase transition (see figure 5 (*a*)) because of a sudden increase in the spontaneous polarization at the transition temperature. The relaxation frequencies of the various modes versus temperature are shown in figure 5 (*b*).

3.2.3. *FiLC phase (101°C < T < 103°C)*

A three dimensional dielectric spectrum of the material with frequency and temperature as variables is given in figure 6 (*a*) to provide visual observations of the various modes. In the absence of a d.c. bias voltage, one strong relaxation at low frequency (200 Hz) is observed. Figure 6 (*b*) shows dielectric loss, ε , spectra in greater detail for a bias voltage $V = 0$ V; at different temperatures. The magnitude of ε increases when the sample is heated from 101 to 104°C. This may be due to an increase in $\mathbf{P}_S$ occurring as a consequence of a rapid change in structure with temperature in this region, reminiscent of the FiLC phase. An increase in ε may arise from large fluctuations in the structure originating from a perturbation by the small measuring electric field (~100 mV) across the cell. The phase in this temperature interval is assigned to the FiLC phase as found from $\mathbf{P}_S$ measurements. This was

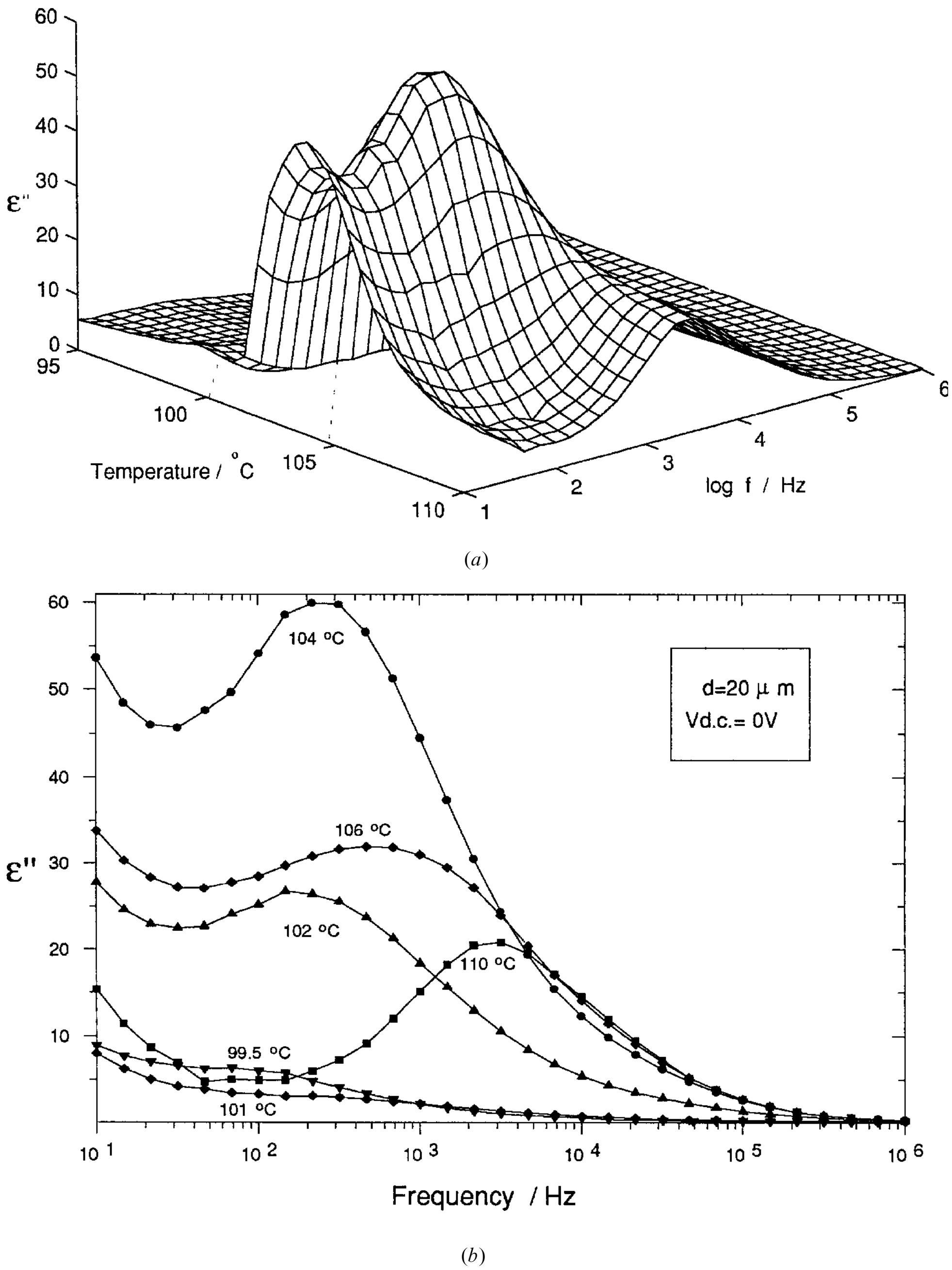

Figure 6. (a) 3-D plot of ε versus temperature and frequency. The *ferri* Goldstone mode (200 Hz) occurs in SmC_γ and FiLC phases; the *ferro* Goldstone mode (3 kHz) is found in the $T=105$–110°C temperature range. (b) Dielectric loss ε versus frequency for d.c. bias voltage $V=0$ V; ε is a maximum in the FiLC phase (due to a ferrielectric Goldstone mode).

labelled as Fi2 phase in the DSC trace obtained on heating.

The low frequency mode with a relaxation frequency centred at approximately 200 Hz is labelled as *ferri* Goldstone mode, see figure 6(*b*) at $T=102$°C. This assignment is given because it (a) occurs in both the ferrielectric SmC_γ and FiLC phases, (b) has a low frequency and (c) is quite easily suppressed by the applied field. This mode is about a decade lower in frequency than the *ferro* Goldstone mode (3 kHz) in the SmC* phase. The ferrielectric Goldstone mode has also been reported in the literature [11–15] in other antiferroelectric samples.

The dielectric strength $\Delta\varepsilon_{\mathrm{ferri}}$ of the *ferri* Goldstone mode is found to increase rapidly with temperature (see figure 5(*a*)) within the FiLC phase. This increase in dielectric strength may be associated with a rapid change in the polarization, associated with the instability of the phase with $q_T=3/5$ which would cause the spontaneous polarization to increase. An increase in the pitch (p_O) of the ferrielectric helix due to increasing temperature could also cause an increase in the dielectric strength. The peak occurring in the dielectric strength just below the FiLC–SmC* phase transition is probably due to a maximum in the ferrielectric pitch at that temperature. This maximum may mark the temperature above which coexistence of FiLC and SmC* phases is observed.

The electric field dependence of the dielectric strength of the *ferri* Goldstone mode was examined under d.c. bias voltage. The dielectric strength $\Delta\varepsilon$ versus temperature at a bias voltage of 1 V is shown in figure 7 (*a*). The dielectric strength in the FiLC phase is reduced due to the bias field. In the SmC_γ phase, application of a small d.c. bias voltage 2 V causes a small increase in the dielectric strength across the cell (see figure 7 (*b*)). This behaviour may be due to an increase in the ferroelectric character (ordering) of the SmC_γ phase. For bias voltages 2 V however, the dielectric strength is reduced. The freedom of the director fluctuations (in azimuthal angle φ) around the tilt cone is reduced with increasing bias voltage and this also distorts the helix that is present in the structure. The net result is the suppression of the strength of the *ferri* Goldstone relaxation mode.

In the FiLC phase however, the behaviour of the dielectric strength with applied field is markedly different from that in the SmC_γ. Application of a bias voltage drastically reduces the dielectric strength of this

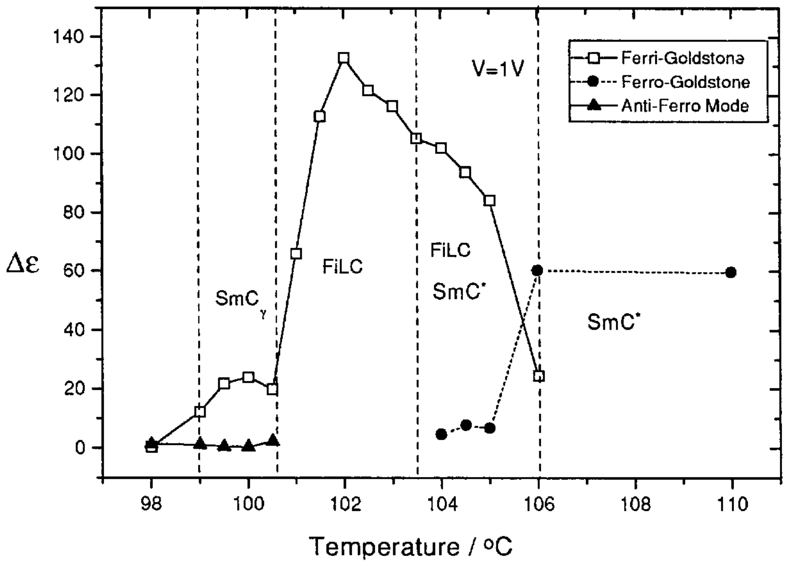

(*a*)

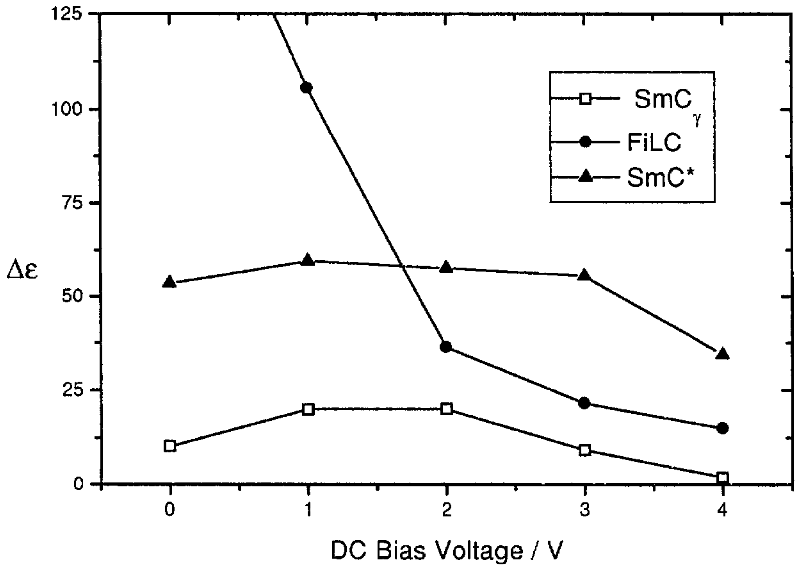

(*b*)

Figure 7. (*a*) The dielectric strength $\Delta\varepsilon$ versus sample temperature, for d.c. bias voltage $V = 1$ V. (*b*) The dielectric strength $\Delta\varepsilon$ versus d.c. bias voltage for the Goldstone mode in ferrielectric FiLC, SmC_γ and SmC* phases.

relaxation. The dielectric strength $\Delta\varepsilon_{ferri}=180$ for zero bias voltage is reduced to $\Delta\varepsilon_{ferri}\approx20$ for a bias of 4 V, see figure 7 (*b*). For a d.c. bias voltage of 4 V applied across the cell, the low frequency *ferri* mode is completely suppressed and the FiLC phase is transformed into SmC* as shown in figure 8. The low frequency ferrielectric mode disappears and instead the ferroelectric Goldstone mode in the SmC* phase is observed. This is in line with the results of $\mathbf{P}_S$ measurements for large applied electric fields (>1 V μm^{-1}); the ferrielectric FiLC phase is transformed completely to the ferroelectric SmC* phase, see figure 2.

3.2.4. *Coexistence of FiLC and SmC* phases (103°C< T<106°C)*

From DSC data, the phase transition from FiLC to SmC* occurs at $T=103$°C. In the temperature range (103°C$<T<$106°C) two relaxation modes are found to exist. These modes correspond to the *ferri* and *ferro* Goldstone modes. At a temperature $T=106$°C ($V_{d.c.}>0$ V) a low frequency ferrielectric Goldstone mode is found to exist, see figure 8. The broad peak shown in figure 8, (d.c. bias=0 V) indicates the coexistence of the FiLC and SmC* phases. The contributions of ferrielectric and ferroelectric modes to ε at $T=106$°C is reflected in the broad curve shown in figure 6 (*b*).

3.2.5. *Ferroelectric SmC* phase (106°C< T<121°C)*

The effects of bias voltage on the ferroelectric Goldstone mode relaxation at $T=110$°C are shown in figure 9. For a d.c. bias voltage $V=0$ V, the ferroelectric Goldstone relaxation mode is detected in the SmC* phase. For an applied voltage 0 V$<V<$2 V, the dielectric loss ε shows the unusual property of increasing slightly (see figure 9). This we believe is due to the transformation of the smectic layer structure from chevron to bookshelf. For the bookshelf structure, there is no layer tilting with respect to the normal to the plane of the cell-electrodes. Thus the component of the spontaneous polarization across the electrodes will be higher than in the case of tilted smectic layers (chevron). For d.c. bias voltages $V>2$ V, the Goldstone mode is suppressed by d.c. bias as normally found in the SmC* phase (see figure 8).

3.2.6. *Thermal hysteresis in the dielectric loss spectra*

Thermal hysteresis is observed in ε spectra of the sample between the heating and cooling cycles, see figure 10. This reflects a complex dependence of the stability of the phase sequence on the direction of the temperature change. The large low frequency (100 Hz–1 kHz) ε peak occurring in the FiLC phase ($T=104$°C) found in the heating cycle is not observed in the cooling cycle, see figure 10. This behaviour is explained because, on heating, the ground state is the antiferroelectric state and hence an increase in the temperature induces an increase in ferroelectric ordering. Thus the temperature induced staircase as suggested by the Ising model is observed. The ferrielectric phase FiLC with $q_T=3/5$ (similar to $q_E=4/5$) is clearly observed on heating (large dielectric peak at 200 Hz). The ferroelectric ordering is reduced on cooling from a stable ferroelectric phase with $q_T=1$. However, the antiferroelectric ordering is now destabilized by the initial and subsequent preference for ferroelectric ordering, and thus the proper temperature induced devil's staircase is not observed. Indeed the transition between SmC* and SmC_A appears to occur abruptly on cooling. The phase change, e.g. SmC_A–SmC_γ–FiLC, (coexistence of FiLC and SmC*),

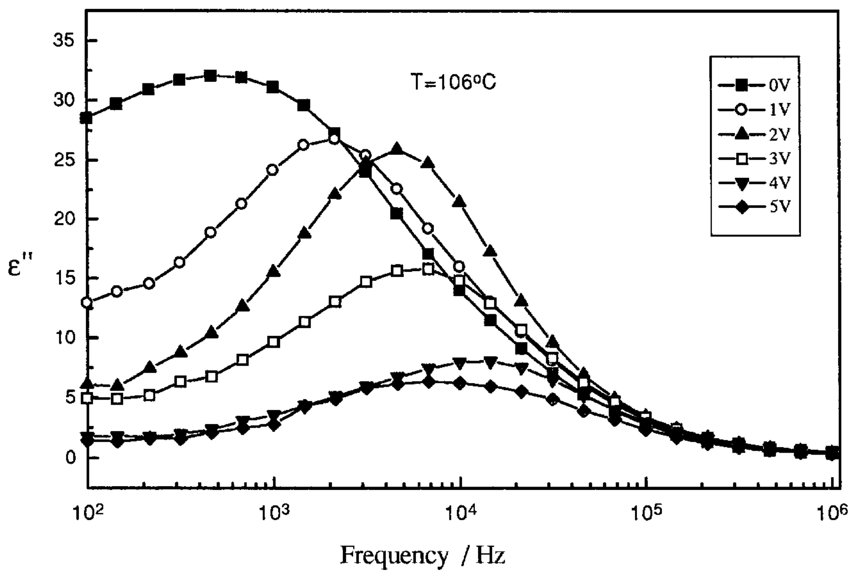

Figure 8. The dielectric loss ε versus frequency at $T=106$°C, for d.c. bias voltages of 1, 2, 3, 4, 5 V. The low frequency *ferri* mode (200 Hz) is completely suppressed at V 4 V.

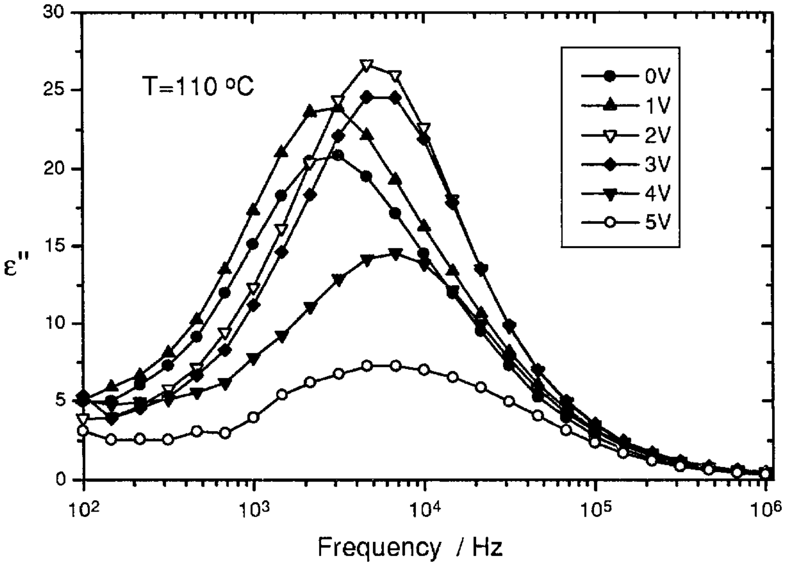

Figure 9. Plot of ε versus frequency at $T = 110°C$, for d.c. bias voltages of 1, 2, 3, 4, 5 V.

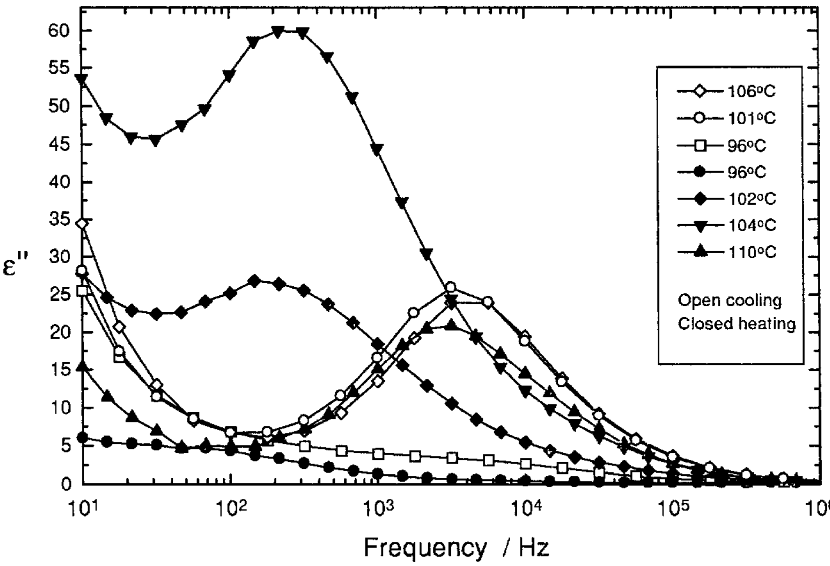

Figure 10. The dielectric loss ε as a function of temperature and frequency during heating and cooling cycles from $T = 95$–110°C, with $V_{d.c.} = 0$ V; open symbols refer to cooling and closed symbols to heating.

SmC*–SmA which occurs on heating, appears as SmA–SmC*–SmC_A on cooling. In the DSC trace, SmC_γ phase was labelled as Fi1 and FiLC phase as Fi2. The reasons for these assignments have been given. The DSC trace also showed a small peak at 106°C probably signifying an end to the coexistence of the two phases seen in the dielectric spectra.

4. Summary

The results are summarised as follows:

(i) One stable ferrielectric state SmC_γ and a ferrielectric phase (FiLC) are found from the spontaneous polarization measurements. There is also evidence of a field induced FiL phase existing over a narrow range of electric fields. The FiL phase is not observed on thermal cycling (i.e. temperature induced staircase).

(ii) The temperature dependence of the hysteresis of the spontaneous polarization with applied field ($T = 98°C$, 93°C), indicates competition between the temperature induced and field induced devil's staircases.

(iii) In the SmC_A phase two relaxation modes were observed, *Process A* and *Process B*. In the SmC_γ and FiLC phases a *ferri* Goldstone mode (≈200 Hz) was found. The dielectric strength is highest in the FiLC phase because the structure of this phase is fluctuating and can easily be disturbed by external fields; a small change in applied field can cause a large change in the polarization. The normal ferroelectric Goldstone mode ($f \approx 3$ kHz) was observed in the SmC* phase.

(iv) The dielectric strength of the *ferri* Goldstone mode in FiLC was found to decrease substantially for small bias fields (0·05–0·25 V μm^{-1}). This is possibly due to the electric field induced transitions from FiLC to SmC* phase.

(v) Over a certain range of temperatures (between 103 and 106°C), evidence for the coexistence of the ferrielectric FiLC and ferroelectric SmC* phases is found from the dielectric spectra. A small peak in the DSC thermogram signifies an end to this coexistence.

(vi) Thermal hysteresis is observed between the dielectric spectra on heating and cooling. On heating, the ferrielectric *ferri* Goldstone mode (in both SmC_γ and FiLC phases) is observed; on the contrary however it is not found on cooling.

5. Conclusions

The effects of bias voltage and temperature on the polarization and dielectric properties of an antiferroelectric liquid crystal material have been examined. The spontaneous polarization measurements show clear competition between the field induced and temperature induced devil's staircases. The results reveal the existence of an FiLC phase in this antiferroelectric liquid crystal material and confirm a recent discovery of this phase in other AFLC samples [6–8, 15]. The phase is found to be sensitive to external fields and can be classified as rather unstable, in line with the predictions of the Ising model. A field induced FiL state was also found. In an FiLC phase, a low frequency (200 Hz) Goldstone mode was observed and its dielectric strength is dramatically reduced by the application of a small bias voltage. This is due to a low threshold electric field required for inducing a transformation of the FiLC to SmC* phase. The evidence for the coexistence of the FiLC and SmC* phases is also found from the dielectric spectra.

The authors are most obliged to Drs M. Hird and A. J. Seed of the University of Hull, U.K. for having supplied a DSC thermogram of this sample using their most up to date machine. We also thank Dr Yu. P. Panarin for useful discussions. The work was funded partly by EU network CT930353 and partly by Forbairt, Ireland.

References

[1] Fukuda, A., Takanishi, Y., Isozaki, T., Ishikawa, K., and Takezoe, H., 1994, *J. mater. Chem.*, **4,** 997.
[2] Žekš, B., and Čepič, M., 1993, *Liq. Cryst.*, **14,** 445.
[3] Vaksman, V. M., and Panarin, Yu. P., 1992, *Mol. Mat.*, **1,** 147.
[4] Havriliak, S. (Jr), and Negami, S., 1966, *J. Poly. Sci. C*, **14,** 99.
[5] Bak, P., and Von Boem, J., 1980, *Phys. Rev. B*, **21,** 5297.
[6] Hatano, J., Hanakai, Y., Furue, H., Uehara, H., Saito, S., and Murashiro, K., 1994, *Jpn. J. appl. Phys.*, **33,** 5498.
[7] Panarin, Yu. P., Xu, H., MacLughadha, S. T., Vij, J. K., Seed, A. J., Hird, M., and Goodby, J. W., 1995, *J. Phys. Condens. Matter*, **7,** L351.
[8] O'Sullivan, J. W., Panarin, Yu. P., Vij, J. K., Seed, A. J., Hird, M., and Goodby, J. W., 1996, *J. Phys. Condens. Matter*, **8,** L551.
[9] Buivydas, M., Gouda, F., Lagerwall, S. T., and Stebler, B., 1995, *Liq. Cryst.*, **18,** 879.
[10] Hiraoka, K., Takezoe, H., and Fukuda, A., 1993, *Ferroelectrics*, **147,** 13.
[11] Gisse, P., Pavel, J., Nguyen, H. T., and Lorman, V. L., 1993, *Ferroelectrics*, **147,** 27.
[12] Bibonne, F., Parneix, J. P., Isaert, N., Joly, G., Nguyen, H. T., Bouchta, A., and Destrade, C., 1995, *Mol. Cryst. liq. Cryst.*, **263,** 27.
[13] Hiller, S., Pikin, S. A., Haase, W., Goodby, J. W., and Nishiyama, I., 1994, *Jpn. J. appl. Phys.*, **33,** 1096.
[14] Čepič, M., Heppke, G., Hollidt, J. M., Lötzsch, D., and Žekš, B., 1993, *Ferroelectrics*, **147,** 159.
[15] Panarin, Yu. P., Kalinovskaya, O., Vij, J. K., and Goodby, J. W., 1997, *Phys. Rev. E*, **55,** 4345.